

Identification of network-level coding units for real-time representation of episodic experiences in the hippocampus

Longnian Lin^{*†§}, Remus Osan^{*†§}, Shy Shoham[‡], Wenjun Jin^{*†}, Wenqi Zuo^{*†}, and Joe Z. Tsien^{*†¶}

^{*}Center for Systems Neurobiology, Departments of Pharmacology and Biomedical Engineering, Boston University, Boston, MA 02118; [†]Shanghai Institute of Brain Functional Genomics, East China Normal University, Shanghai 200062, China; and [‡]Department of Molecular Biology, Princeton University, Princeton, NJ 08544-1014

Edited by Thomas C. Südhof, University of Texas Southwestern Medical Center, Dallas, TX, and approved March 1, 2005 (received for review November 4, 2004)

To examine the network-level organizing principles by which the brain achieves its real-time encoding of episodic information, we have developed a 96-channel array to simultaneously record the activity patterns of as many as 260 individual neurons in the mouse hippocampus during various startling episodes. We find that the mnemonic startling episodes triggered firing changes in a set of CA1 neurons in both startle-type and environment-dependent manners. Pattern classification methods reveal that these firing changes form distinct ensemble representations in a low-dimensional encoding subspace. Application of a sliding window technique further enabled us to reliably capture not only the temporal dynamics of real-time network encoding but also postevent processing of newly formed ensemble traces. Our analyses revealed that the network-encoding power is derived from a set of functional coding units, termed neural cliques, in the CA1 network. The individual neurons within neural cliques exhibit “collective cospiking” dynamics that allow the neural clique to overcome the response variability of its members and to achieve real-time encoding robustness. Conversion of activation patterns of these coding unit assemblies into a set of real-time digital codes permits concise and universal representation and categorization of discrete behavioral episodes across different individual brains.

episodic memory | neural clique | neural code | startle | cell assembly

Understanding the network-level organizing principles that allow the brain to form real-time neural representations of episodic experiences is a central issue in neuroscience. Anatomically, the hippocampus, and especially its CA1 subregion, is known to be a crucial site for the formation of episodic memories of events and places (1–6). In fact, individual hippocampal neurons have been shown to respond to many external inputs (7–13). Yet, the response variability at the level of individual neurons poses a theoretical obstacle to the understanding how the brain achieves its robust real-time neural coding of the stimulus representation (14–16). It has been long thought that mnemonic encoding of information may involve the coordinated activity of large numbers of individual neurons (17, 18). However, virtually little is known about the actual real-time network-level encoding patterns and their underlying organizing principles and mechanisms.

To study these issues, we have developed a high-density recording technique for mice in which sophisticated genetic analyses of cognitions are feasible (19, 20). In parallel, we have also designed a set of simple, and yet robust, behavioral paradigms by using startling episodes. We reasoned that such episodic events are likely to involve large numbers of neurons, thereby greatly increasing the chance of finding them simultaneously and, consequently, facilitating the analysis of network-level real-time encoding patterns in the brain. Here, we report on our experimental measurements and mathematical descriptions of CA1-encoding patterns associated with various mne-

monic startling episodes, as well as on the identification of functional coding units, termed neural cliques, in the hippocampal network. Furthermore, we describe a way to convert the real-time activation patterns of neural clique assemblies to an invariant binary code for categorizing and representing episodic information across different individual brains.

Materials and Methods

In Vivo Recording and Spike Sorting. The 96-channel recording array (in stereotrode format) was constructed and implanted onto the head of B6BCA/J mice. The electrodes were advanced slowly until reaching the CA1. The spike activities in freely behaving mice in response to various startling episodes such as an air blow to the animal’s back, free fall of the animal while inside a small elevator, or earthquake-like cage shake were recorded by Plexon Systems (Dallas) and then sorted by using the MCLUST3.0 and KLUSTAKWIK 1.5 programs (21). Only stable units (for at least 6 h) with clear boundaries and <0.5% of spike intervals within a 1-ms refractory period are included in the present analysis.

Data Analysis. The firing rates of each neuron during the 1 s that followed the startle stimuli were computed by using two 500-ms time bins ($f_{\text{poststartle}, n}$). The neural responses were obtained by using $R_n = (f_{\text{poststartle}, n} - f_{\text{pre}})/(f_o + f_{\text{pre}})$, where f_{pre} is the prestimulus baseline firing rate and f_o is the global mean response frequency of the recorded excitatory neuron (2–3 Hz). Multiple discriminant analysis (MDA) (22) was used to compute a highly informative low-dimensional subspace that allows discriminating among the different startling episodes. Projections of training data points in this subspace were fit with multivariate Gaussian distributions:

$$P(x) = \frac{1}{(2\pi)^{N/2} |\Sigma|^{1/2}} \exp(- (x - m)^T \Sigma^{-1} (x - m) / 2)$$

to compute prediction of class membership for test data points (leave-one-out method). Hierarchical clustering (22) was used to group neurons with similar response properties as a way of identifying encoding units in CA1. The MDA ensemble responses were then mapped into a startle-selective encoding coordinate system to obtain efficient and universal binary codes for categorizing startle episodes across different animals.

For a detailed description of construction of 96-channel ensemble recording array (Fig. 6, which is published as support-

This paper was submitted directly (Track II) to the PNAS office.

Abbreviation: MDA, multiple discriminant analysis.

§L.L. and R.O. contributed equally to this work.

¶To whom correspondence should be addressed. E-mail: jtsien@bu.edu.

© 2005 by The National Academy of Sciences of the USA

ing information on the PNAS web site), *in vivo* recording and spike sorting (Figs. 7 and 8, which are published as supporting information on the PNAS web site), behavioral tests of startling memories, and data analysis, please see *Supporting Text*, which is published as supporting information on the PNAS web site.

Results

Ensemble Patterns of CA1 Single-Unit Activity Triggered by Startling Events. Because the brain can produce robust episodic memories of startling events (e.g., devastating earthquakes, roller coaster rides, shark attack, etc.) even upon a single exposure (23–25), we have correspondingly designed a set of behavioral paradigms and used three different types of startling stimuli delivered to the mice as a way of creating discrete episodic startle memories: air blow, a sudden blow of air to the animal's back (mimicking an owl attack from sky); drop, a short vertical free fall inside a small elevator (recreating the mouse's experiences inside a cookie jar that falls from a kitchen shelf); and shake, an unexpected brief earthquake-like shaking of the mouse's cage. We used computer-controlled mechanical devices for controlling the precise timing and intensity of these startling stimuli. Such startling episodic events are capable of producing robust startle memories, as evident from our measurements of the 3-h retention of place conditioning memory (Fig. 9, which is published as supporting information on the PNAS web site).

We simultaneously recorded 260, 210, 148, and 138 individual CA1 units in mice A, B, C, and D, respectively, while subjecting them to seven repetitions of each of the above-mentioned startling stimuli. These stimuli produced collective changes in firing rates and activity patterns within a subset of the recorded neuronal populations. As an example, the spike rasters of 260 simultaneously recorded single units from mouse A show dynamical changes in the firing patterns of many CA1 neurons after the occurrence of single startling episodes of air blow, drop, and shake (Fig. 1).

Diversity in CA1 Cell Response Selectivity to Startling Episodes. To analyze the neural basis underlying the formation of episodic memory, we first examined the temporal dynamics of each individual CA1 cell in response to a variety of startling events. Although a significant proportion of the simultaneously recorded CA1 cells did not respond to any of the startle stimuli, the remainder exhibited significant changes in firing rates. In general, based on their temporal response duration, dynamical changes triggered by startling episodes can be generally divided into four major firing modes: transient increase, transient decrease, prolonged increase, and prolonged decrease (see Fig. 10, which is published as supporting information on the PNAS web site). The transient changes were as short as 250 ms or less, whereas the prolonged increases lasted up to 40 s in duration.

Of the total of 756 single units recorded (pooled from four animals), 13.5% exhibited transient increases, 31.7% showed prolonged increases, 1.9% had transient decreases, and 1.4% responded with a prolonged decrease in their firing frequency. Thus, the ratio of neurons showing increased vs. decreased firing is ≈ 14 to 1. We further note that although the spike discharge frequency and interspike-intervals of these individual neurons were quite variable across repetitions (for several examples, see peri-event spike rasters in Fig. 2; see also Fig. 10), response modes to the same type of startle were almost always consistent in terms of their temporal dynamics (i.e., transient vs. prolonged, increase vs. decrease).

We then analyzed the response-selectivity of these CA1 cells. Spike-raster plots and peri-event histograms reveal that some of these CA1 neurons responded to all three types of startling events (Fig. 2*A*, general startle cells), whereas other cells appeared to only respond to air blow, drop, or shake (Fig. 2*B–D*). Importantly, we have also observed many CA1 cells that

reacted to combinations of two different types of startles, responding to both startles either equally or differentially (Fig. 2*E* and *F*), thereby reflecting the hippocampal binding function of cortical inputs. This diversity of response-specificity suggests that the startling events are likely to be represented in CA1 by activity patterns of unique ensembles of neurons.

Effects of Environmental Contexts on Startle-Induced Individual Neuronal Responses. Because the hippocampus is involved in the formation of episodic memory that contains not only “what” information but also “where” information (1–5, 8), we next asked to what extent the firing patterns of CA1 cells triggered by startling events are influenced by the environmental contexts in which the startles occur. To address this question, we repeated the sudden air blow stimuli in two distinct cages and the drop stimuli in two different elevators. Although a given type of startling stimuli triggered similar responses in many of the responsive CA1 units regardless of the environmental context (Fig. 2*G* and *H*), some CA1 cells exhibited context-specific firing changes (Fig. 2*I* and *J*). Thus, these contextual experiments demonstrate that the startle-triggered firing changes in some CA1 neurons are not only stimulus-dependent, but also depend on the context in which the event occurs, thereby reflecting a clear neural integration of both what and where information in

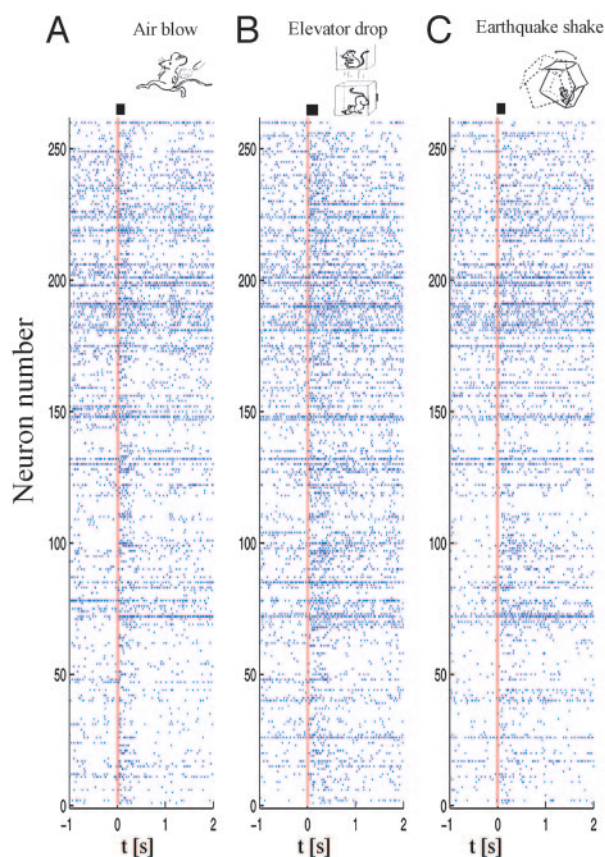


Fig. 1. Startle-induced ensemble of single-unit firing patterns in CA1. Spike rasters of 260 simultaneously recorded single units from mouse A during a period of 1 s before and 2 s after the occurrence of single startling episodes of air blow (*A*), drop (*B*), and shake (*C*) ($t = 0$ marked with vertical red line). *x* axis, time scale (seconds); *y* axis, the numbers of simultaneously recorded single units ($n = 260$). The startle stimulus durations are indicated as a bar next to the vertical red line above the spike raster. Although many neurons did not respond to startling stimuli, a significant portion of recorded units exhibited dynamical changes in their firing rates.

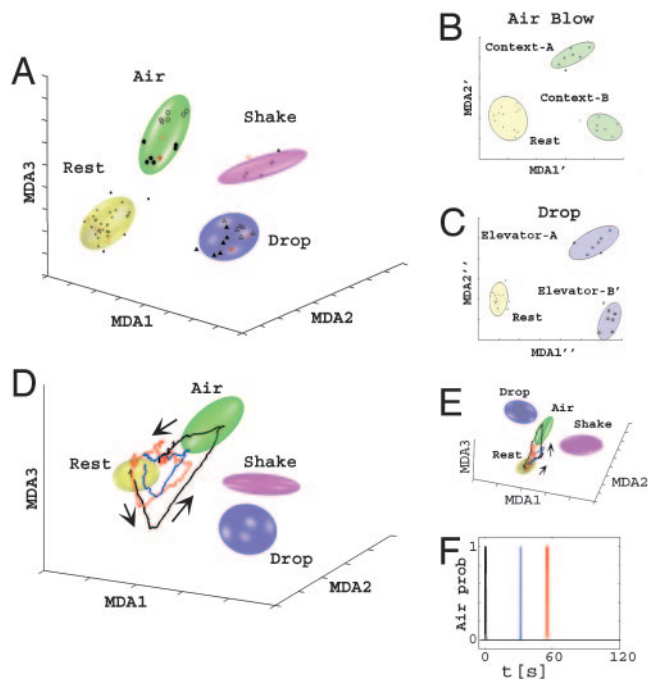


Fig. 3. Classification, visualization, and dynamical decoding of CA1 ensemble representations of startle episodes by MDA methods. (A) Firing patterns during rest (dots, yellow ellipsoid), air blow (circles, green ellipsoid), drop (triangles, blue ellipsoid), and shake (stars, magenta ellipsoid) epochs are shown after being projected to a three-dimensional space obtained by using MDA for mouse A; MDA1–3 denote the discriminant axes. Both training (dark symbols) and test (red symbols) data are shown. After the identification of startle types, a subsequent MDA is further used to resolve contexts (full vs. empty symbols) in which the startle occurred for air-blow context (B) and for elevator drop (C). (D) Dynamical monitoring of ensemble activity and the spontaneous reactivation of startle representations. Three-dimensional subspace trajectories of the population activity in the two minutes after an air-blow startle in mouse A are shown. The initial response to an air blow (black line) is followed by two large spontaneous excursions (blue and red lines), characterized by coplanar, geometrically similar lower amplitude trajectories (directionality indicated by arrows). (E) The same trajectories of A from a different 3D angle. (F) The timing ($t_1 = 31.6$ s and $t_2 = 54.8$ s) of the two reactivations (marked in blue and red, respectively) after the actual startle (in black) ($t = 0$ s). The vertical axis indicates the air-blow classification probability.

Monitoring of Real-Time Encoding and Dynamical Postevent Processing of CA1 Network Traces. MDA provides a sensitive and mathematical means of measuring and visualizing the ensemble neural activity patterns in a highly informative encoding subspace. This dimensionality-reduction method can further be used to dynamically monitor the population firing patterns by using a sliding-window technique (1-s width; see *Supporting Text*). Using

the fixed matrix coefficients produced by the MDA method, we can compute the instantaneous projection of neural responses during the entire experiment. As such, the temporal evolution of the ensemble activity patterns can be directly visualized as dynamical trajectories in the encoding subspace. For example, during the baseline state before startles, the instantaneous projection was confined to the rest ellipsoid; however, upon the actual startling stimulus, we observe a planar trajectory that begins in the rest cluster, quickly visits the corresponding startle cluster, and then returns to rest (an example for air blow is shown in Fig. 3 D–F, and for drop, black trajectories, see Fig. 12, which is published as supporting information on the PNAS web site).

Intriguingly, using this approach, we further observed spontaneous excursions from the rest ellipsoid during the poststartling event period (Fig. 3D). These intrinsic excursions occurred in all four animals and had the directional specificity as well as the characteristic geometric shape of the original startle trajectories. Moreover, their spontaneous trajectories took place on the similar time scale and were also confined in the same plane but typically with a smaller magnitude than the startle-evoked trajectories (Fig. 3D and E, red and blue trajectories for reactivations after an air-blow episode). We also measured the time of these spontaneous excursions, which were observed to occur causally at several seconds to minutes, with apparently random intervals, after the actual startles (Fig. 3F). For example, the timing of the two reactivations after the actual air-blow startle shown in Fig. 3D is $t_1 = 31.6$ s (red trajectories) and $t_2 = 54.8$ s (blue trajectories) (Fig. 3F), whereas the timing of a reactivation in another case (drop) is at 107.9 seconds (Fig. 12). The number of reactivations that followed the original startles ranged between zero and five in our experiments. Therefore, our analyses have allowed us to monitor the dynamics of postevent spontaneous reactivations and processing of CA1 ensemble patterns.

Identification of Functional Coding Units, Neural Cliques, in the CA1 Network. Our finding that the representations of startle events form tight, well separated clusters in a low-dimensional encoding subspace prompted us to examine in detail which neurons in the CA1 population are responsible for encoding the different events and what essential features of the neural signals are used to accomplish that. Thus, we used agglomerative hierarchical clustering (22), a pattern classification method that can aggregate units by iteratively grouping together neurons with minimally distant responses. The clustering results reveal the existence of various neural groups, or neural cliques, with similar response properties (Fig. 4A). These neural cliques exhibited an increase in firing rate to all three types of startles (i.e., a “general startle clique”), to one type of startle (i.e., “air-blow clique,” “drop clique,” and “shake clique”), and to a subset of mixed startles (i.e., drop/shake clique, drop/air-blow clique, and air-blow/shake clique), respectively.

How significant a role do these neural cliques play in CA1 encoding classification? We evaluated the contribution of these

Table 1. Prediction power in the MDA-computed encoding subspace for startle type and context

Mouse	Rest	Air blow	Air blow in context A	Air blow in context B	Drop	Drop in elevator A	Drop in elevator B	Shake
A	99	99	99	94	99	91	98	98
B	99	99	94	95	97	92	93	93
C	99	99	91	92	99	80	87	90
D	99	90	91	75	96	66	75	83

Percent correct predictions were evaluated by using 1,000 random combinations of training/test data for each mouse. Test data was excluded from the training set. The startle type was first determined (columns: rest, air blow, drop, and shake), followed by context classification for air blow (context A or B) and drop (elevator A or B). Data sets contained 260, 210, 148, and 138 simultaneously recorded CA1 units in mice A, B, C, and D, respectively.

to the specificity exhibited by neural cliques, this MDA subspace does not show startle-type selectivity along any of its discriminant axes. To translate the ensemble responses into a startle-selective encoding coordinate system, we assigned new positions for the cluster centers so that they are linearly mapped into a clique-space, where each axis directly corresponds to a particular clique, thus projecting specific activation patterns to 1 and the absence of activation to 0. This mathematical operation achieves the reorientation of the main axes of the low-dimensional encoding subspace by inverting the matrix containing the centers of startle representations in that space (see *Supporting Text* for the matrix inversion step).

By projecting the ensemble patterns directly into this clique space, the recorded neural activities are now mapped onto a set of highly reproducible and selective responses. Each clique-space projection vector (columns in Fig. 5A) is clearly selective to a specific combination of startles (i.e., general-startle, air blow, drop, etc.), and does not respond to additional features. In addition, this selectivity also extends to the representation of contexts. Furthermore, the weights in the projection vectors strongly correlate with the responsiveness of neurons in the corresponding clique (data not shown). As a result, the activated cliques can be directly detected by using simple threshold crossing and, consequently, their collective identity uniquely codes for any given startle. For example, based on a predefined sequence of clique assembly (general-startle/air blow/drop/shake/air subcontext/drop subcontext), the activation code 110010 corresponds to the internal representation of the air blow in context A, 110000 to air blow in context B, 101000 to drop elevator A, 101001 to drop elevator B, and 100100 to shake.

Importantly, these binary codes can be dynamically implemented to detect the occurrence of the internal representations of startling episodes. For example, using the thresholded responses of these cliques, we can compute the “hit ratio” for correctly matching activation patterns with the binary codes. The prediction performance obtained by using these codes are the same to the ones listed in Table 1 (see also Table 4, which is published as supporting information on the PNAS web site).

Identification of neural cliques as the functional coding units for internal representation has prompted us to further look into the robustness of real-time encoding by neural cliques. This finding is a particularly important issue, as it is well known that a single neuron often shows large variations in both spike discharge and interspike intervals in response to repetition of identical stimuli (14–16). We found that these individual members within each clique fired tightly together in close temporal proximity during startle episodes. This collective cospiking feature allowed the neural cliques to overcome the response variability of their individual members and, thus, to achieve real-time encoding robust-

ness. For example, the neural clique formed by the 10-drop neurons used in Fig. 4 consistently produced robust response to drops, but not to air blow or shake events (Fig. 5B). Further examination of their temporal dynamics at finer time scale (20–30 ms) again confirmed that the collective cospiking of these individual neurons has greatly enhanced real-time signal-to-noise robustness (Fig. 13, which is published as supporting information on the PNAS web site). Therefore, the cospiking of clique neurons is capable of providing a network-level mechanism for real-time encoding robustness and can act as a robust internal timer to reliably signal the occurrence of external events.

Discussion

A central issue in the study of neural coding in the brain is the response variability of individual neurons (14–16). This variability at the level of individual neurons has posed a theoretical challenge for understanding how the brain achieves its real-time encoding and decoding of behavioral experiences. A traditional way to deal with this issue is to average the response of an individual neuron over many repetitions and trials. Although it allows the identification of event-related neural response, this practice of data averaging unfortunately loses crucial information regarding real-time neural coding functions. Here, we have described and visualized the network-level encoding patterns and postevent immediate processing of startling episodic experience in the CA1 region of the hippocampus. We have further identified network-level functional coding units capable of overcoming the response variability of individual neurons and achieving real-time network representation of startling episodic experiences. It would be of interest to investigate how the individual neurons that comprise a functional coding clique are anatomically connected and how they are modulated by synaptic plasticity (26–28), and to further dissect to what extent they reflect the sensory, emotional, mnemonic, or even conceptual aspects of the events (7, 23). Nonetheless, when the activation patterns of these coding units are converted (29) into a set of concise digital codes, they seem to permit universal representation and categorization of discrete behavioral episodes across different animals. Therefore, the “neural clique cospiking” principle provides a plausible network-level basis by which the nervous systems can achieve real-time neural coding and processing of behavioral information. For more discussion on our findings, see *Extended Discussion* in *Supporting Text*.

We thank Yuan Liu and Kim Zaia for assistance and Dr. Gyorgy Buzsaki and his staff for providing advice on the ensemble recordings. This research was supported by funds from National Institutes of Health Grants MH60236, MH61925, MH62632, and AG02022, the Burroughs Wellcome Fund, ECNU Award TY04610, Ministry of Science and Technology of China Program Project 973, and the W. M. Keck Foundation (all to J.Z.T.).

1. Squire, L. R. (1987) *Memory and Brain* (Oxford Univ. Press, Oxford).
2. Cohen, N. J. & Eichenbaum, H. (1993) *Memory, Amnesia, and the Hippocampal System* (MIT Press, Cambridge, MA).
3. Rudy, J. W., Barrientos, R. M. & O'Reilly, R. C. (2002) *Behav. Neurosci.* **116**, 530–538.
4. Rampon, C., Tang, Y. P., Goodhouse, J., Shimizu, E., Kynin, M. & Tsien, J. Z. (2000) *Nat. Neurosci.* **3**, 238–244.
5. Sara, S. J. (2000) *Learn. Mem.* **7**, 73–84.
6. Wittenberg, G. M. & Tsien, J. Z. (2002) *Trends Neurosci.* **25**, 501–505.
7. Berger, T. W., Alger, B. & Thompson, R. F. (1976) *Science* **192**, 483–485.
8. O'Keefe, J. & Nadal, L. (1978) *The Hippocampus as a Cognitive Map* (Oxford Univ. Press, Oxford).
9. Weiss, C., Kronforst-Collins, M. A. & Disterhoft, J. F. (1996) *Hippocampus* **6**, 192–209.
10. Deadwyler, S. A., Bunn, T. & Hampson, R. E. (1996) *J. Neurosci.* **16**, 354–372.
11. Wilson, M. A. & McNaughton, B. L. (1994) *Science* **265**, 676–679.
12. Wirth, S., Yanike, M., Frank, L. M., Smith, A. C., Brown, E. N. & Suzuki, W. A. (2003) *Science* **300**, 1578–1581.
13. Dragoi, G., Harris, K. D. & Buzsaki, G. (2003) *Neuron* **39**, 843–853.
14. Lestienne, R. (2001) *Prog. Neurobiol.* **65**, 545–591.
15. Abbott, L. F. & Dayan, P. (1999) *Neural Comput.* **11**, 91–101.
16. Fenton, A. A. & Muller, R. U. (1998) *Proc. Natl. Acad. Sci. USA* **95**, 3182–3187.
17. Hebb, D. O. (1949) *The Organization of Behavior* (Wiley, New York).
18. Abbott, L. E. & Sejnowski, T. J. (1999) *Neural Codes and Distributed Representations* (MIT Press, Cambridge, MA).
19. Shimizu, E., Tang, Y. P., Rampon, C. & Tsien, J. Z. (2000) *Science* **290**, 1170–1174.
20. Wang, H., Shimizu, E., Tang, Y.-P., Cho, M., Kynin, M., Zuo, W., Robinson, D. A., Alaimo, P. J., Zhang, C., Morimoto, H., et al. (2003) *Proc. Natl. Acad. Sci. USA* **100**, 4287–4292.
21. Scicsvari, J., Hirase, H., Czurko, A. & Buzsaki, G. (1998) *Neuron* **21**, 179–189.
22. Duda, R. O., Hart, E. P. & Stork, D. G. (2001) *Pattern Classification* (Wiley, New York).
23. Koch, M. (1999) *Prog. Neurobiol.* **59**, 107–128.
24. Davis, M., Hitchcock, J. & Rosen, J. B. (1987) *The Psychology of Learning and Memory*, ed. Bower, G. H. (Academic, New York).
25. LeDoux, J. E. (1994) *Sci. Am.* **270**, 50–57.
26. Wigstrom, H. & Gustafsson, B. (1985) *Acta Physiol. Scand.* **123**, 519–522.
27. Malenka, R. C. & Nicoll, R. A. (1999) *Science* **285**, 1870–1874.
28. Tsien, J. Z. (2000) *Sci. Am.* **282**, 62–68.
29. McCulloch, W. S. & Pitts, W. (1943) *Bull. Math. Biol.* **52**, 99–115.